Acta Pharmacologica Sinica

www.nature.com/aps

ARTICLE

Autophagy inhibitors increase the susceptibility of KRAS-mutant human colorectal cancer cells to a combined treatment of 2-deoxy-D-glucose and lovastatin

Xiao-ming Huang[1], Jia-jun Huang[1], Jing-jing Du[1], Na Zhang[1], Ze Long[1], You Yang[1], Fang-fang Zhong[1], Bo-wen Zheng[1], Yun-fu Shen[1], Zhe Huang[1], Xiang Qin[1], Jun-he Chen[1], Qian-yu Lin[1], Wan-jun Lin[1] and Wen-zhe Ma[1]

RAS-driven colorectal cancer relies on glucose metabolism to support uncontrolled growth. However, monotherapy with glycolysis inhibitors like 2-deoxy-D-glucose causes limited effectiveness. Recent studies suggest that anti-tumor effects of glycolysis inhibition could be improved by combination treatment with inhibitors of oxidative phosphorylation. In this study we investigated the effect of a combination of 2-deoxy-D-glucose with lovastatin (a known inhibitor of mevalonate pathway and oxidative phosphorylation) on growth of KRAS-mutant human colorectal cancer cell lines HCT116 and LoVo. A combination of lovastatin (>3.75 μM) and 2-deoxy-D-glucose (>1.25 mM) synergistically reduced cell viability, arrested cells in the G_2/M phase, and induced apoptosis. The combined treatment also reduced cellular oxygen consumption and extracellular acidification rate, resulting in decreased production of ATP and lower steady-state ATP levels. Energy depletion markedly activated AMPK, inhibited mTOR and RAS signaling pathways, eventually inducing autophagy, the cellular pro-survival process under metabolic stress, whereas inhibition of autophagy by chloroquine (6.25 μM) enhanced the cytotoxic effect of the combination of lovastatin and 2-deoxy-D-glucose. These in vitro experiment results were reproduced in a nude mouse xenograft model of HCT116 cells. Our findings suggest that concurrently targeting glycolysis, oxidative phosphorylation, and autophagy may be a promising regimen for the management of RAS-driven colorectal cancers.

Keywords: human colorectal cancers; lovastatin; 2DG; glycolysis; OXPHOS; autophagy; chloroquine; hydroxychloroquine

Acta Pharmacologica Sinica (2021) 42:1875–1887; https://doi.org/10.1038/s41401-021-00612-9

INTRODUCTION

Despite recent advances in diagnosis and prevention, colorectal cancer (CRC) accounted for an estimated 9,600,000 deaths (9.2% of the total cancer deaths) and 18,100,00 new cases (10.2% of the total cancer cases) worldwide in 2018 [1]. Approximately 40% and 3%–5% of CRCs exhibit activating oncogenic driver mutations in the KRAS and NRAS genes, respectively [2]. Currently, patients with CRCs with RAS mutations are treated by a multimodal approach modified according to tumor-specific characteristics but generally consisting of surgical resection followed by chemotherapy or immunotherapy with monoclonal antibodies. However, the use of chemotherapy and monoclonal antibodies is associated with severe side effects and drug resistance [3]. Therefore, new treatment regimens are urgently needed.

Mutated RAS proteins promote metabolic reprogramming characterized by glucose dependence, which provides an attractive therapeutic target in RAS-driven CRCs [4]. However, treatment with 2-deoxy-D-glucose (2DG), the most widely investigated glycolysis inhibitor, either alone or in combination with other cytotoxic drugs, was shown to have limited favorable clinical results [5, 6]. The failure of 2DG may be the result of a compensatory increase in oxidative phosphorylation (OXPHOS) metabolism triggered when glycolysis is inhibited. Moreover, in recent years, accumulating evidence has revealed that several cancers also exhibit significant or even enhanced OXPHOS capacity [7]. Therefore, simultaneously targeting both glycolysis and OXPHOS has been suggested as a potential treatment approach for certain types of cancer [8, 9]. The combination of 2DG with metformin, a widely prescribed antidiabetic drug that with anticancer activity that is induced through the inhibition of mitochondrial complex I, was shown to synergistically inhibit cancer cell growth and metastasis [10–12].

Statins are a class of lipid-lowering drugs used to reduce cholesterol synthesis by blocking 3-hydroxy-3-methylglutaryl coenzyme-A (HMG-CoA) reductase in the mevalonate pathway, a metabolic cascade that also plays an essential role in tumorigenesis. This mechanism of action may be particularly relevant for CRCs, for which hyperlipidemia is among the key risk factors [13]. Geranyl pyrophosphate (GPP) and farnesyl pyrophosphate (FPP), the intermediate products of the mevalonate pathway, are required for RAS prenylation and membrane translocation, which trigger oncogenic signal transduction [14]. While statins have been extensively investigated for possible applications in cancer management, their use remains controversial. Findings to date have been ambiguous and even contradictory [15], possibly because of treatment is not targeted to particular tumor types and

[1]State Key Laboratory of Quality Research in Chinese Medicine, Macau University of Science and Technology, Macau, China
Correspondence: Wen-zhe Ma (wzma@must.edu.mo)

Received: 16 September 2020 Accepted: 9 January 2021
Published online: 19 February 2021

because of the development of resistance to statin monotherapy in these studies [15]. Statins are known to induce mitochondrial dysfunction, which is manifested as statin-associated muscle symptoms (SAMS), the most common side effect of statins [16, 17]. We proposed that, similar to metformin, statin-mediated inhibition of mitochondria may be leveraged to treat cancers susceptible to OXPHOS inhibition. Therefore, it is suggested that statins may be more effective in treating RAS-driven CRCs when used in combination with a glycolysis inhibitor.

Autophagy is a conserved cellular process in which damaged intracellular components are catabolized. It plays a number of complicated roles in cancer, being either tumor suppressive or tumor promoting under different circumstances [18]. Monotherapy with the autophagy inhibitors chloroquine (CQ) or hydroxychloroquine (HCQ), which are currently used for the treatment of malaria and inflammatory conditions, has shown promise in clinical trials for various types of cancer [19]. In addition, the combination of CQ/HCQ with chemotherapy or radiation also elicits a better treatment response [20]. Autophagy provides substrates for energy production and promotes cell survival under stress conditions, such as during adenosine triphosphate (ATP) depletion caused by the inhibition of glycolysis or OXPHOS [21]. Therefore, we speculated that the inhibition of autophagy by CQ/HCQ can enhance the anticancer activity of a combination of 2DG and a statin, which has not yet been reported.

The HCT116 and LoVo KRAS-mutant CRC cell lines have been widely used in CRC research. In this study, we tested the anticancer activity of the combination of lovastatin and 2DG on these two KRAS-mutant cell lines. We also investigated the effect of a combination treatment on autophagy, and we measured cell susceptibility upon autophagy inhibition. Our study provides a metabolic regimen for RAS-mutant CRC treatment that simultaneously disrupts three major intracellular energy-producing pathways by inhibiting glycolysis, OXPHOS, and autophagy.

MATERIALS AND METHODS

Cell lines and culture conditions

The HCT116 and LoVo KRAS-mutant human CRC cell lines, the HCT-8 KRAS wild-type human CRC cell line and the HEK293T human embryonic kidney cell line were purchased from ATCC (Manassas, VA, USA). The CCD-841-CoN human normal colonic epithelial cell line was a kind gift from Prof Lin Li at the Institute of Biochemistry and Cell Biology, Chinese Academy of Sciences, Shanghai, China. The HCT116, LoVo, and HEK293T cells were cultured in Dulbecco's modified Eagle's medium (DMEM; Gibco, NY, USA), whereas the HCT-8 and CCD-841-CoN cells were cultured in RPMI-1640 (Gibco, NY, USA) supplemented with 10% fetal bovine serum (FBS; Gibco, NY, USA), 100 units/mL penicillin and 100 mg/mL streptomycin at 37 °C and 5% CO_2.

Chemicals

Lovastatin (Sigma Aldrich, St. Louis, MO, USA) was dissolved in dimethyl sulfoxide (DMSO; Acros Organics, Morris Plains, NJ, USA) and stored at −40 °C. 2-Deoxy-D-glucose (Alfa Aesar, Haverhill, MA, USA) was dissolved in the culture medium. Sulforhodamine B (SRB), trichloroacetic acid (TCA), puromycin, carbonyl cyanide phospho-(p)-trifluoromethoxy phenylhydrazone (FCCP), farnesyl pyrophosphate ammonium salt (FPP), oligomycin, rotenone, antimycin A, Tris base, and crystal violet were purchased from Sigma Aldrich (St. Louis, MO, USA), and bafilomycin A1, CQ, mevalonic acid lithium salt (MVA), actinomycin D (AD), and HCQ were purchased from MedChemExpress (Monmouth Junction, NJ, USA).

Antibodies

Primary antibodies against human proteins: rabbit monoclonal anti-cleaved caspase-3 (#9664), rabbit monoclonal anti-cleaved poly (ADP ribose) polymerase (anti-PARP) (#5625), rabbit polyclonal anti-AMP-activated protein kinase α (anti-AMPKα) (#2532), rabbit monoclonal anti-phospho-AMPK α (anti-p-AMPKα) (#2535), rabbit monoclonal anti-mammalian target of rapamycin (anti-mTOR; #2983), rabbit polyclonal anti-phospho-mTOR (anti-p-mTOR; #2974), rabbit monoclonal anti-phospho-ribosomal protein S6 kinase (anti-p-p70 S6K; #9234), rabbit monoclonal anti-p70 S6K (#2708), rabbit monoclonal anti-p-4E-binding protein 1 (anti-p-4E-BP1; #2885), rabbit monoclonal anti-4E-BP1 (#9644), rabbit monoclonal anti-Beclin-1 (#3495), rabbit monoclonal anti-p-cell division cycle 2 (anti-p-cdc2; #4539), rabbit monoclonal anti-cyclin B1 (#12231), rabbit polyclonal anti-extracellular signal-regulated kinase (anti-ERK; #9102), rabbit polyclonal anti-p-ERK (anti-p-ERK; #9101), rabbit polyclonal anti-AKT (#9272), mouse monoclonal anti-cyclin A2 (#4656), and mouse monoclonal anti-p-AKT (p-AKT; #4051) were from Cell Signaling Technology (Beverly, MA, USA). Rabbit polyclonal anti-p-tyrosine-independent ligand for the Lck SH2 domain of 62 kDa (anti-p62) antibody (#155686) was purchased from Abcam (Cambridge, MA, USA), and rabbit polyclonal anti-microtubule-associated protein 1 A/1B-light chain 3 (anti-LC3; #L8918) and mouse monoclonal anti-β-actin antibodies (#A5441) were purchased from Sigma (St. Louis, MO, USA). Anti-mouse (#715-035-150) and anti-rabbit (#211-035-109) secondary antibodies were purchased from Jackson ImmunoResearch Laboratories (West Grove, PA, USA).

Cell cycle analysis

Cells were seeded in six-well plates at a density of 2×10^5 cells/mL and treated with the indicated drugs for 24 h. The cells were trypsinized, harvested, washed twice with phosphate-buffered saline (PBS), fixed using 70% ethanol at −20 °C for 2 h, and stained with 500 μL PI (50 μg/mL)/RNase A (200 μg/mL; KeyGen Biotech, Nanjing, China) for 30 min at room temperature. The cells were subsequently pelleted, washed, and resuspended in PBS at a final concentration of 1×10^6/mL. The data were acquired from 10,000 events detected using a FACSAria II flow cytometry apparatus (BD Bioscience, San Jose, CA, USA) and analyzed by FlowJo software (Tree Star, Ashland, OR, USA) using the Dean-Jett-Fox model.

Cell proliferation assay

Cell proliferation assays were performed using SRB, as previously described [22]. Cells (5×10^4 cells/mL) were seeded in 96-well plates at a volume of 100 μL per well and incubated overnight. After incubation, 100 μL of medium containing the indicated drugs was added. The cells were fixed with 50 μL of cold 50% (*w*/*v*) trichloroacetic acid (TCA) at 4 °C for 1 h and subsequently stained with 0.4% (*w*/*v*) SRB at room temperature for 30 min. The OD_{515nm} was determined using a SpectraMax paradigm microplate reader (Molecular Devices, Sunnyvale, CA, USA) following the addition of 200 μL of 10 mM Tris base solution (pH 10.5).

Combination index analysis

Cells (5×10^3) were seeded in 96-well plates and treated with a range of concentrations of lovastatin and 2DG, alone or in combination, for 72 h. Cell proliferation was determined, and the combination index (CI) was calculated using CompuSyn software (Version 1.0; T. C. Chou and N. Martin, Memorial Sloan-Kettering Cancer Center, New York, USA), as previously described [23]. The combined effect of lovastatin and 2DG was determined based on the CI value, where $CI < 1$ represents a synergic effect, $CI = 1$ represents an additive effect, and $CI > 1$ represents antagonism. An isobologram was generated using CompuSyn software to visually represent the drug synergism, additivity, and antagonism [24].

Colony formation assay

Cells were plated at 1000–2500 cells/well density in 6-well plates one day prior to treatment with the indicated drugs and

incubated for 7–15 d. Surviving colonies were washed with PBS, stained with 0.2% (*w*/*v*) crystal violet in 4% formalin (Sigma Aldrich, St. Louis, MO, USA) for 10 min and photographed using a GelDoc XR Imaging System (Bio-Rad, Hercules, CA, USA). The colony numbers (diameter > 50 μm) were counted using ImageJ software (Bethesda, MD, USA).

Annexin V/PI staining

Cell apoptosis was analyzed with a FITC Annexin V Apoptosis Detection Kit I (BD Bioscience, San Jose, CA, USA) via FACSAria II flow cytometry (BD Bioscience, San Jose, CA, USA). Cells were plated at a density of 2×10^5 cells/well in 6-well plates one day prior to treatment with the indicated drugs. After 48 h of treatment, the cells were harvested, washed with cold PBS, resuspended in 100 μL of 1× binding buffer, stained with 2.5 μL of FITC Annexin V and 2.5 μL PI, and incubated for 15 min in the dark at room temperature. The cells were filtered, and the data were acquired from 10,000 events with a FACSAria II flow cytometer within 1 h. The data were analyzed using FlowJo software (Tree Star, Ashland, OR, USA) to determine the total number of apoptotic cells.

Seahorse XFp respirometry assay

The oxygen consumption rate (OCR) and extracellular acidification rate (ECAR) of HCT116 cells were measured with a Seahorse XFp real-time ATP rate assay kit according to the manufacturer's protocol using an XFp extracellular flux analyzer (Seahorse Bioscience, Billerica, MA, USA). Cells were seeded at 5×10^3 cells/well in XFp cell culture miniplates and treated with the indicated drugs. After incubation for 48 h, the cells were washed and incubated in the XF assay medium at 37 °C in a CO_2-free incubator for 1 h. OCR and ECAR were automatically recorded and calculated using Seahorse XFp software (Seahorse Bioscience, Billerica, MA, USA), and the ATP production rates were calculated using ECAR and OCR measurements as previously described [25].

Determination of intracellular ATP level

Cells were seeded at 2×10^5 cells/well in a 12-well plate in duplicate, with one well used for the ATP assay and the other will used for the protein assay. Following overnight incubation, the cells were treated with the indicated drugs for 24 h and washed once with PBS before being harvested. ATP concentration was measured using an ATP determination kit (Molecular Probes, Eugene, OR, USA). Finally, the steady-state intracellular ATP levels were normalized to the protein concentration and reported as nmol/mg protein.

Western blotting

Cells were plated in six-well plates and treated with the indicated drugs for the indicated time periods. Protein samples were collected in RIPA buffer with protease inhibitor cocktail (Roche, Mannheim, Germany) and phosphatase inhibitor (Roche, Mannheim, Germany). The samples were boiled at 95 °C for 5 min after dilution in protein loading buffer. Samples containing 20 μg of protein were loaded on sodium dodecyl sulfate-polyacrylamide (SDS-PAGE) gels. After fractionation on SDS-PAGE gels, the proteins were transferred to polyvinylidene difluoride (PVDF) membranes (Millipore, Billerica, MA, USA) and incubated overnight with primary antibodies at 4 °C. The membranes were washed with 1× Tris buffered saline with 0.1% Tween 20 (1× TBST) and incubated with the appropriate horseradish peroxidase (HRP)-conjugated secondary antibody at room temperature. The proteins were visualized, and the band intensities were quantified using an Amersham Imager 600 (GE Healthcare Life Sciences, Marlborough, MA, USA) with Super-Signal West Pico chemiluminescent substrate or SuperSignal West Dura extended duration substrate (Thermo Scientific, San Jose, CA, USA).

Confocal microscopy

Confocal fluorescent images were captured using a Zeiss LSM SP8 laser confocal microscope (Zeiss LSM, Oberkochen, Germany). Cells were cultured on 35-mm glass-bottom dishes (Cellvis, Mountain View, CA, USA). For the autophagy puncta formation assay, HCT116 cells were stably transfected with pEGFP-LC3 plasmid (Addgene plasmid #21073) and treated with the indicated drugs for 48 h prior to imaging with a 40× oil objective with a GFP filter. For determining the lysosome pH in HCT116 cells, LAMP1-GFP lentivirus was transfected into HCT116 cells 24 h prior to treatment with the indicated drugs for 48 h. The cell medium was subsequently changed to fresh medium with 75 nM LysoTracker Red DND-99 (Invitrogen, Carlsbad, CA, USA), and the cells were incubated for 15 min under cell culture conditions, washed twice with fresh medium, and imaged with a 40× oil objective with GFP and RFP filters.

Lentiviral transduction and stable cell line generation

FUGW-PK-hLC3 (Addgene plasmid #61460) and pLenti-CMV-LAMP1-GFP (PPL#PPL01692-4a) lentiviral constructs were used to express pHluorin-mKate2-hLC3 and LAMP1-GFP in the HCT116 cells, respectively. To generate lentivirus, HEK293T cells were plated at 1×10^6 cells/well in 6-well plates and incubated overnight before being transfected with FUGW-PK-hLC3/pLenti-CMV-LAMP1-GFP (0.5 μg), psPAX (0.375 μg), and pMG2.0 G (0.125 μg) in 50 μL of Opti-MEM (Gibco, NY, USA) with 3 μL of FuGENE HD (Promega, Madison, WI, USA). The transfection mixture was incubated for 10 min at room temperature and then added dropwise to the cells. After 16 h, the medium containing the transfection mixture was replaced with fresh medium. After an additional 48 h, supernatants were collected, filtered through 0.45-μm filters, and directly added to target cells or stored at −80 °C for later use. Lentiviral transduction was performed in the presence of 8.0 μg/mL polybrene. After overnight incubation, the viral transduction medium was exchanged with fresh medium. The cells transduced with the FUGW-PK-hLC3 plasmid, which lacks an antibiotic selection marker in mammalian cells but emits pHluorin (green) and mKate2 (red) fluorescence, were sorted to obtain pHluorin (green) and mKate2 (red) double-positive cells using FACSAria II flow cytometry (BD Bioscience, San Jose, CA, USA) after an additional 48 h, and single-cell clones were isolated by limiting dilution. The cells transduced with the pLenti-CMV-LAMP1-GFP plasmid were selected with 2.0 μg/mL puromycin to generate GFP-positive cells for 7 d before the isolation of single clones.

Autophagic flux assay

The lentivirus derived from FUGW-PK-hLC3 was transduced into HCT116 cells to generate autophagic flux reporter (AFR) cell lines. AFR cells were subsequently subjected to the indicated treatments, washed, trypsinized, and resuspended in 0.5% BSA/PBS for analysis of pHluorin (green) and mKate2 (red) fluorescence by FACSAria II flow cytometry (BD Bioscience, San Jose, CA, USA). The mKate2/pHluorin ratio was generated using BD FACSDiva software 6.0 (San Jose, CA, USA), and the gates were set for low/intermediate/high populations and maintained throughout the experiments.

Xenograft assay

Female BALB/c athymic nude mice (4–6 weeks old) were subcutaneously injected in both hind limbs with 2×10^6 HCT116 cells suspended in 100 μL of PBS. The nude mice were gavaged with lovastatin (25 mg/kg every 2 d), 2DG (5 mg/kg every 2 d), HCQ (80 mg/kg every 2 d) alone, a combination of lovastatin and 2DG or the three drugs when the tumor size reached 100 mm^3. CMC-Na (Acros Organics, Morris Plains, NJ, USA) was used as a control. The length and width of the tumors were measured using a digital caliper, and the volumes were calculated following the equation $\text{volume} = (\text{length} \times \text{width}^2)/2$. All animal experiments

were carried out following the guidelines of the Division of Animal Control and Inspection (DACI) of the Department of Food and Animal Inspection and Control (DFAIC) of Macau and approved by the Animal Care and Use Committee (ACUC) of the Macau University of Science and Technology (MUST).

Statistical analysis

The data are shown as the mean ± SD unless otherwise indicated. Statistical analyses were performed by unpaired two-tailed Student's *t* test using GraphPad Prism 8.0.2 software (San Diego, CA, USA). The data were analyzed by one-way analysis of variance (ANOVA) when more than two groups were compared (* represents $P < 0.05$ and **represents $P < 0.01$). Tukey's test was performed to further analyze the difference when the F ratio was found to be significant.

RESULTS

The combination of lovastatin and 2DG synergistically inhibits the proliferation of KRAS-mutant CRC cells

To determine the effect of the combination of lovastatin and 2DG on the growth of KRAS-mutant human CRCs, we treated HCT116 and LoVo cells with a series of lovastatin concentrations ranging from 3.75 μM to 60 μM and 2DG concentrations ranging from 1.25 mM to 20 mM alone or in combination for 72 h. The results indicated that either lovastatin or 2DG inhibited the growth of HCT116 and LoVo cells in a concentration-dependent manner (Fig. 1a). Furthermore, the combination of the two drugs inhibited cell proliferation to a significantly higher degree than the individual treatments (Fig. 1a). The CI values were lower than 1 for all the combinations (except with 3.75 μM lovastatin and 1.25 mM 2DG in the HCT116 cells), indicating a synergistic interaction between lovastatin and 2DG (Fig. 1b and Tables 1 and 2). The isobologram analysis demonstrated the synergistic effects of the combination of lovastatin and 2DG when the fractional effect (Fa, the effective doses of inhibition) was set at 0.5, 0.75, and 0.9 for the HCT116 cells and at 0.5 and 0.75 for the LoVo cells, respectively (Fig. 1c). The colony formation assay confirmed the synergistic effect of the combination of lovastatin with 2DG on cell proliferation of both the HCT116 and LoVo cells (Fig. 1d). No such synergistic effect was observed in the human CRC cell line HCT-8 with wild-type KRAS (Supplementary Fig. S1a), although treatments with either lovastatin or 2DG alone exhibited similar inhibition rates on cell proliferation as in the KRAS-mutant HCT116 and LoVo cells. In the CCD-841-CoN normal human colonic epithelial cell line, less robust inhibition of cell proliferation was observed compared to that of the CRC cell lines with either the single-drug treatments or the combination drug treatment (Supplementary Fig. S1c).

The combination of lovastatin and 2DG triggers significantly increased apoptosis rates

Since the induction of apoptosis is the most common mechanism underlying the effect of chemotherapeutic drugs on cell proliferation, we next checked whether it is affected by lovastatin and/or 2DG. Monotherapy with either lovastatin or 2DG only resulted in slight (10%) or moderate (20%) increases in Annexin V-positive fractions of HCT116 cells and LoVo cells, respectively (Fig. 2a, b). However, the combination of 2DG and lovastatin significantly increased the apoptosis rate to 24.89% for the HCT116 cells and 50.43% for the LoVo cells ($P < 0.01$; Fig. 2a, b). These results were confirmed by Western blotting, showing an increase in the cleaved forms of caspase-3 and PARP, protein markers of apoptosis (Fig. 2c, d).

Mutation of RAS leads to constitutive activation of the protein and triggers subsequent activation of the oncogenic RAF/MEK1/2/ERK and PI3K/AKT pathways [26]. To investigate whether these signaling pathways were affected by lovastatin and/or 2DG, we examined the protein expression levels of AKT and ERK proteins, as well as their activated phosphorylated forms. Monotherapy with lovastatin did not obviously change the phosphorylation levels of AKT or ERK. In contrast, monotherapy with 2DG significantly decreased the phosphorylation level of ERK in both KRAS-mutant CRC cell lines (Fig. 2e, f). Interestingly, we observed a significant reduction in the levels of phosphorylated AKT and phosphorylated ERK when the cells were treated with the combination of drugs compared to levels measured after single-drug treatments (Fig. 2e, f).

The combination of lovastatin and 2DG induces G_2/M cell cycle arrest

A close relationship exists between the cell cycle and the apoptosis of cancer cells [27]. Therefore, we sought to determine whether treatment with the combination of lovastatin and 2DG regulates the cell cycle distribution of HCT116 and LoVo cells. After 24 h of treatment, a significant increase in the G_2/M fraction and a decrease in the G_0/G_1 fraction were observed in cells treated with the combination of agents compared to the untreated cells and those treated with the single agents (Fig. 3a, b). It was noted that neither 2DG nor lovastatin alone significantly changed the cell cycle progression of HCT116 cells. In the LoVo cells, the G_0/G_1 phase was increased by lovastatin treatment, the fraction in the S phase was decreased by treatment with either lovastatin or 2DG treatment, and the fraction in the G_2/M phase was reduced by treatment with lovastatin (Fig. 3a, b). The cyclin B1/cdc2 complex is essential for the G_2/M transition, and dephosphorylation of Try15 activates the kinase activity of cdc2 [28]. Cyclin A is another crucial enzyme that promotes the entry of cells into mitosis, and its inactivation results in G_2 arrest [29]. In line with the FACS analysis, Western blotting showed that the combination treatment significantly downregulated the levels of p-cdc2 (Try15), cyclin B1, and cyclin A2 more than either drug alone (Fig. 3c, d).

The combination of lovastatin and 2DG depletes the intracellular ATP level and regulates the AMPK/mTOR pathway

Previous research, including work performed by our group, has shown that statins impair mitochondrial respiration by inhibiting the mevalonate pathway in skeletal muscle cells, leading to dysregulated metabolism and contributing to the dominant side effect, SAMS [30]. Thus, we speculated that statins can be used as mitochondrial inhibitors for the potential application in cancer treatment. Indeed, lovastatin significantly decreased the OCR in HCT116 cells, as assessed by the Seahorse metabolic analyzer (Fig. 4a). In line with previously published findings [31], 2DG significantly decreased both the OCR and ECAR (Fig. 4a, b). The combination of lovastatin and 2DG exhibited the most profound effect on both OXHPOS and glycolysis (Fig. 4a, b). As a result, the calculated total ATP production rate was significantly decreased by lovastatin or 2DG treatment, and the combination showed a synergistic effect (Fig. 4c). In the two colon cancer cell lines, the steady-state intracellular ATP levels exhibited similar patterns following treatment with individual agents and the combination treatment (Fig. 4d). The effect of lovastatin, 2DG, and the combination of the two agents on cellular energy metabolism was consistent with their impact on cell growth (Fig. 1). Supplementation with mevalonate, the immediate product of HMG-CoA reductase in the mevalonate pathway, attenuated lovastatin- but not 2DG-induced cell death, as measured by the SRB assay (Fig. 4e). This effect was confirmed by the colony formation assay, which showed that supplementation with FPP, another metabolite in the mevalonate pathway, partially attenuated the cytotoxic effect of lovastatin, similar to the effect of mevalonate supplementation (Fig. 4f).

AMPK is a highly conserved Ser/Thr protein kinase complex that monitors the bioenergetic state of cells [32]. As a result of decreased intracellular ATP levels, AMPK phosphorylation to generate the active form, p-AMPK, was induced by 2DG and

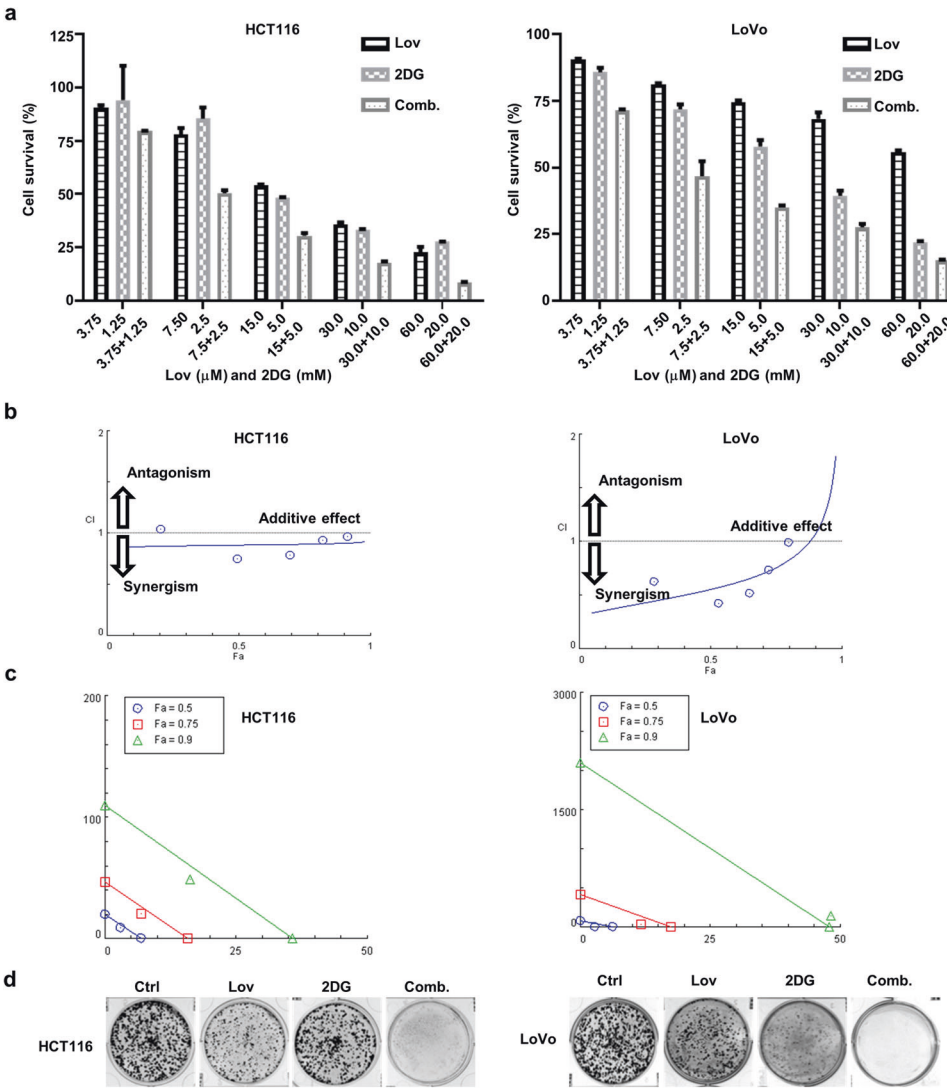

Fig. 1 The combination of lovastatin and 2DG synergistically inhibits the proliferation of KRAS-mutant CRC cells. a HCT116 and LoVo cells were cultured with different concentrations of lovastatin and 2DG alone or in combination for 72 h, and cell proliferation was determined. **b** Combination index (CI) plot. The CI was identified using CompuSyn software, where CI < 1, =1, and >1 indicate the synergism, additive effect, and antagonism, respectively. **c** Isobologram of the combination of two drugs. The combination data (triangle, square, and circle) points on the diagonal line indicate additive effects; the lower left indicates synergism, and the upper right indicates antagonism. **d** Colony formation of HCT116 and LoVo cells treated with lovastatin (7.5 μM) and 2DG (2.5 mM) alone or in combination for 10 d. The data are from at least three independent experiments.

Table 1. CI data for drug combination in HCT116.

Drug combination		Fa	CI
Lov (μM)	2DG (mM)		
3.75	1.25	0.205	1.038
7.5	2.5	0.493	0.749
15.0	5.0	0.694	0.789
30.0	10.0	0.819	0.932
60.0	20.0	0.914	0.970

Synergistic (CI < 1); Additive (CI = 1); Antagonistic (CI > 1).

Table 2. CI data for drug combination in LoVo.

Drug combination		Fa	CI
Lov (μM)	2DG (mM)		
3.75	1.25	0.286	0.629
7.5	2.5	0.533	0.419
15.0	5.0	0.649	0.521
30.0	10.0	0.724	0.738
60.0	20.0	0.798	0.990

Synergistic (CI < 1); Additive (CI = 1); Antagonistic (CI > 1).

lovastatin (Fig. 4g, h). Moreover, a synergistic effect was observed with the combination of the two compounds (Fig. 4g, h). AMPK is known to negatively regulate mammalian target of rapamycin (mTOR), which is a central regulator of cell metabolism [33]. The combination of lovastatin and 2DG markedly decreased mTOR activity, as evidenced by the decreased phosphorylation levels of mTOR and its downstream targets p70S6K and 4E-BP1, compared to the effects of either drug alone (Fig. 4g, h).

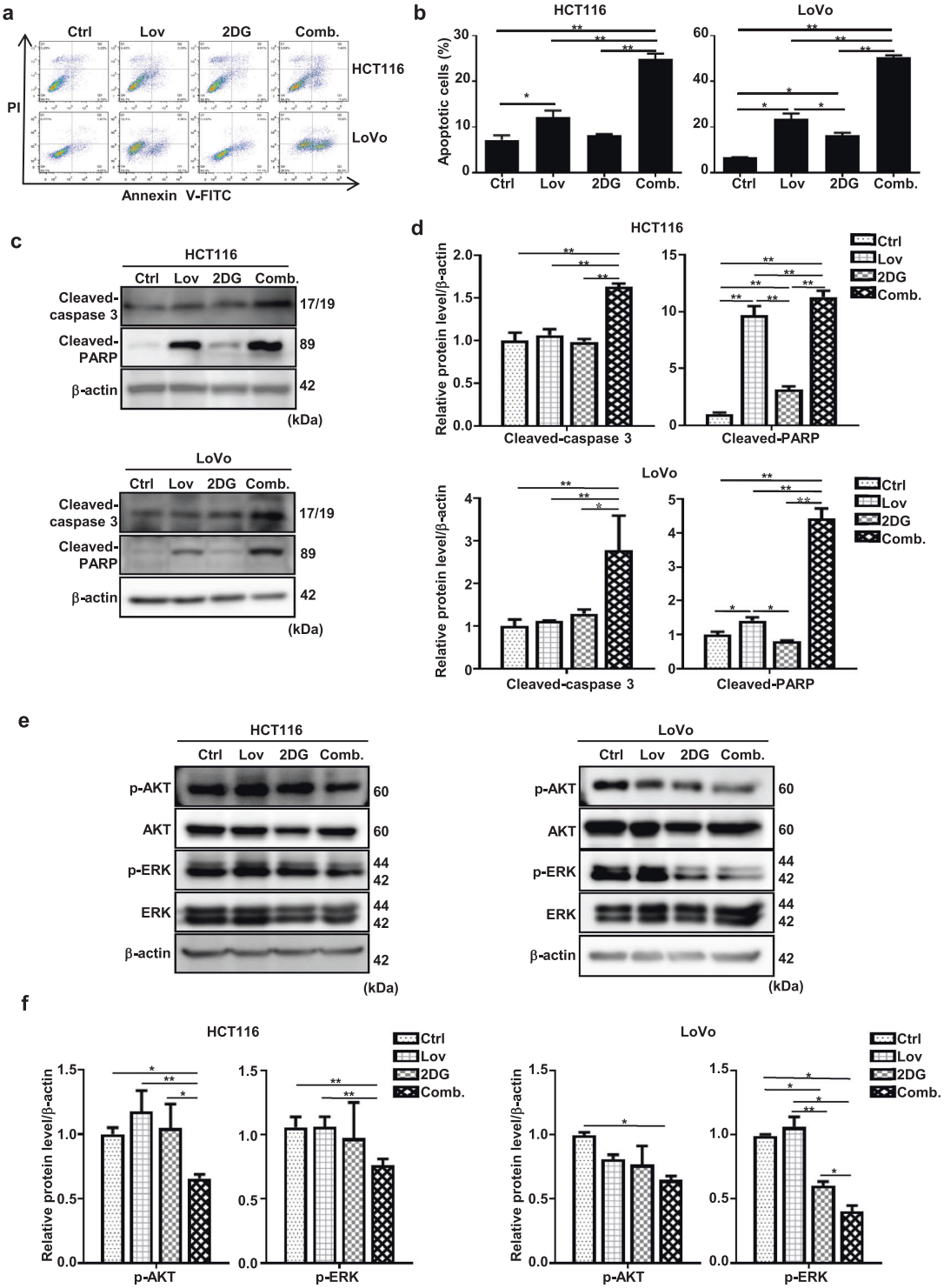

Fig. 2 The combination of lovastatin and 2DG triggers significantly increased apoptosis rates. The combination of lovastatin and 2DG triggers significantly increased apoptosis rates. After treatment with lovastatin (15 μM) and 2DG (5 mM) alone or in combination for 48 h, **a** HCT116 and LoVo cells were stained with FITC Annexin V/PI, and apoptosis was quantified by flow cytometry. **b** Quantification data of the apoptotic cells. **c** Representative immunoblots of cleaved caspase-3 and cleaved PARP in the HCT116 and LoVo cells. β-actin served as a loading control. **d** Quantified data of (**c**). **e** HCT116 and LoVo cells were treated with lovastatin (15 μM) and 2DG (5 mM) alone or in combination for 48 h. Representative immunoblots of AKT, p-AKT, p-ERK, and ERK. β-actin served as a loading control. **f** Quantified data of (**e**). All data are from at least three independent experiments. $^{*}P < 0.05$, $^{**}P < 0.01$.

The combination of lovastatin and 2DG enhances autophagic flux

Autophagy is activated when the activity of mTOR is inhibited [34]. Therefore, we evaluated whether autophagy is affected by the combination of lovastatin and 2DG. The combination of the two drugs significantly increased the LC3II level compared to either drug alone (Fig. 5a, b), which is in line with the observed increase in LC3 puncta (Fig. 5c) and the increased expression of Beclin-1, a known regulator of autophagy (Fig. 5a, b), which dissociates from

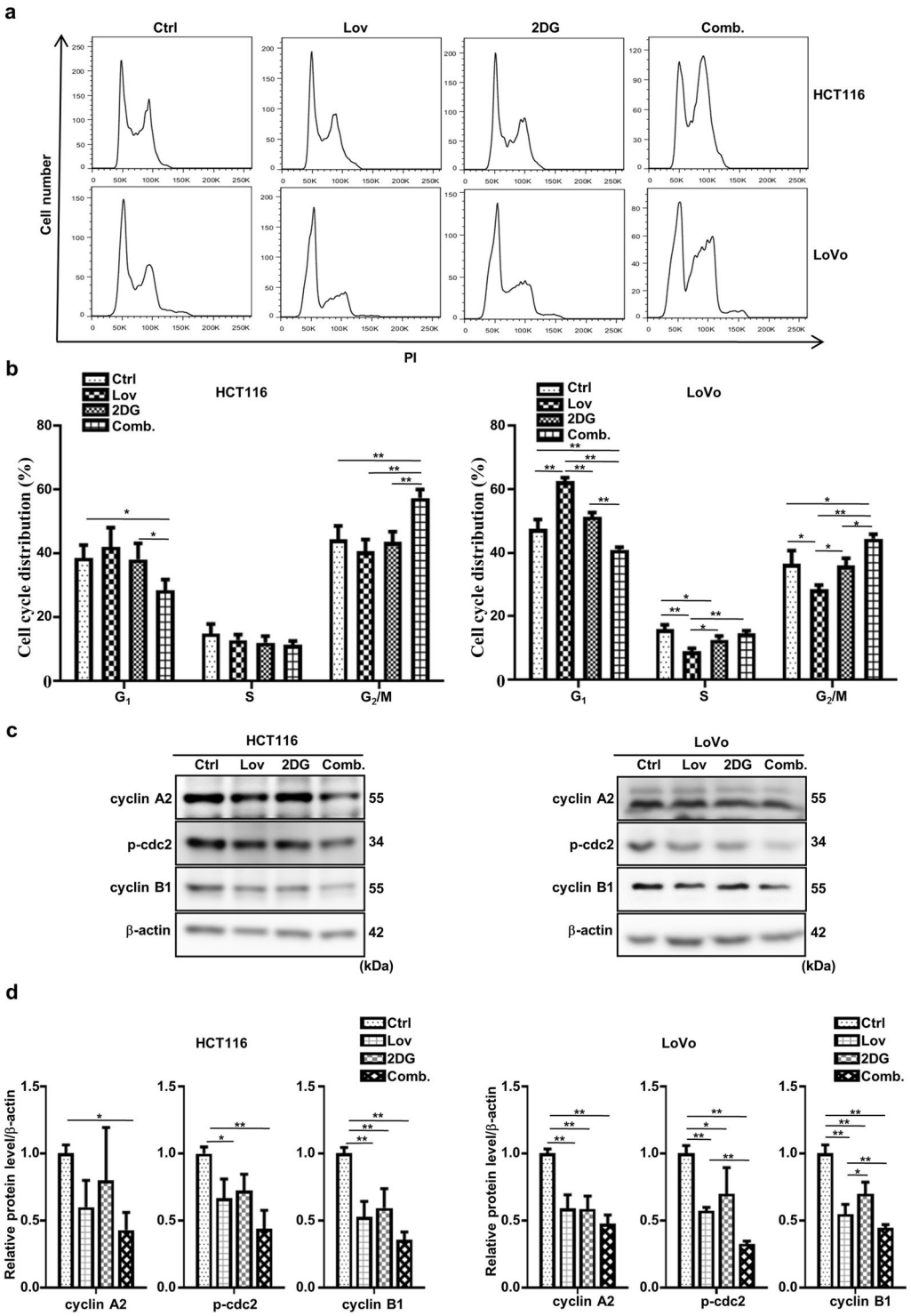

Fig. 3 The combination of lovastatin and 2DG induces G_2/M cell cycle arrest. HCT116 and LoVo cells were treated with lovastatin (15 μM) and 2DG (5 mM) alone or in combination for 24 h. **a** Cell cycle distribution was analyzed using flow cytometry. **b** Percentage of cells in the G_1, S, and G_2/M phase. **c** Representative immunoblots showing the indicated proteins. β-actin served as a loading control. **d** Quantified data of (**c**). All data are from at least three independent experiments. $^*P < 0.05$, $^{**}P < 0.01$.

the Bcl-2/Beclin-1 complex following treatment, as previously reported [35]. Furthermore, lovastatin and 2DG administered individually increased LC3II and Beclin-1 levels in a concentration-dependent manner (Fig. 5d, e). In addition, the accumulation of LC3II and LC-3 puncta may be the result of either the activation of autophagy by enhanced upstream autophagosome formation or the inhibition of autophagy by impaired downstream autophagosome-lysosome degradation [36]. To further clarify this scenario, LC3II levels were measured in the presence of the late-stage autophagy inhibitor bafilomycin A1 (Baf A1), and the results showed a significant increase with treatment with the combination of 2DG and lovastatin (Fig. 5f, g).

The degradation of p62 by lysosomal enzymes is another widely used marker to monitor autophagic flux. However, treatment with

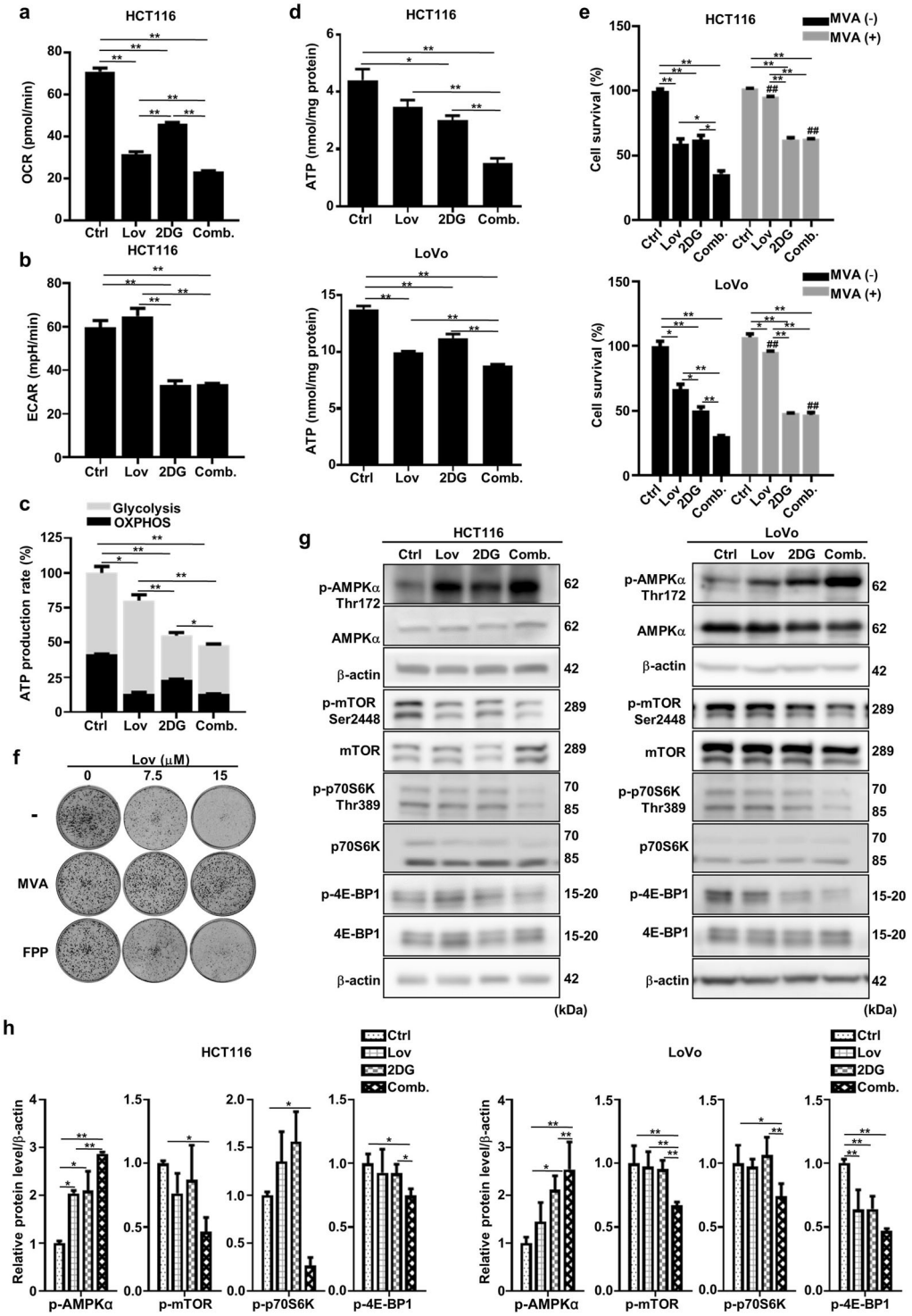

Fig. 4 The combination of lovastatin and 2DG depletes the intracellular ATP level and regulates the AMPK/mTOR pathway. After 48 h of exposure to lovastatin (15 μM) and 2DG (5 mM) alone or in combination, the oxygen consumption rate (**a**) and extracellular acidification rate (**b**) of HCT116 cells were measured on a Seahorse XFp analyzer. **c** The relative ATP production rate by glycolysis and OXPHOS was calculated by measuring oxygen consumption and extracellular acidification with a Seahorse XFp analyzer ($^{*}P < 0.05$, $^{**}P < 0.01$ versus total relative ATP production rate). **d** After treatment with lovastatin (15 μM) and 2DG (5 mM) alone or in combination for 24 h, the intracellular ATP concentrations in HCT116 and LoVo cells were measured. **e** HCT116 and LoVo cells were cultured with lovastatin (15 μM) and 2DG (5 mM) alone or in combination for 72 h in either the presence or absence of 200 mM mevalonate, and cell proliferation was determined. $^{*}P < 0.05$, $^{**}P < 0.01$. $^{\#\#}P < 0.01$ vs corresponding MVA (-) group. **f** HCT116 cells were cultured with lovastatin at the indicated concentrations in the presence or absence of 200 μM mevalonate/10 μM farnesyl pyrophosphate (FPP), and colony formation was determined. **g** Representative immunoblots of AMPKα, p-AMPKα Thr172, mTOR, p-mTOR Ser2448, p70S6K, p-p70S6K Thr389, 4E-BP1 and p-4E-BP1 from the HCT116 and LoVo cells treated with lovastatin (15 μM) and 2DG (5 mM) alone or in combination for 48 h. β-actin served as a loading control. **h** Quantified data of (**g**). All data are from at least three independent experiments.

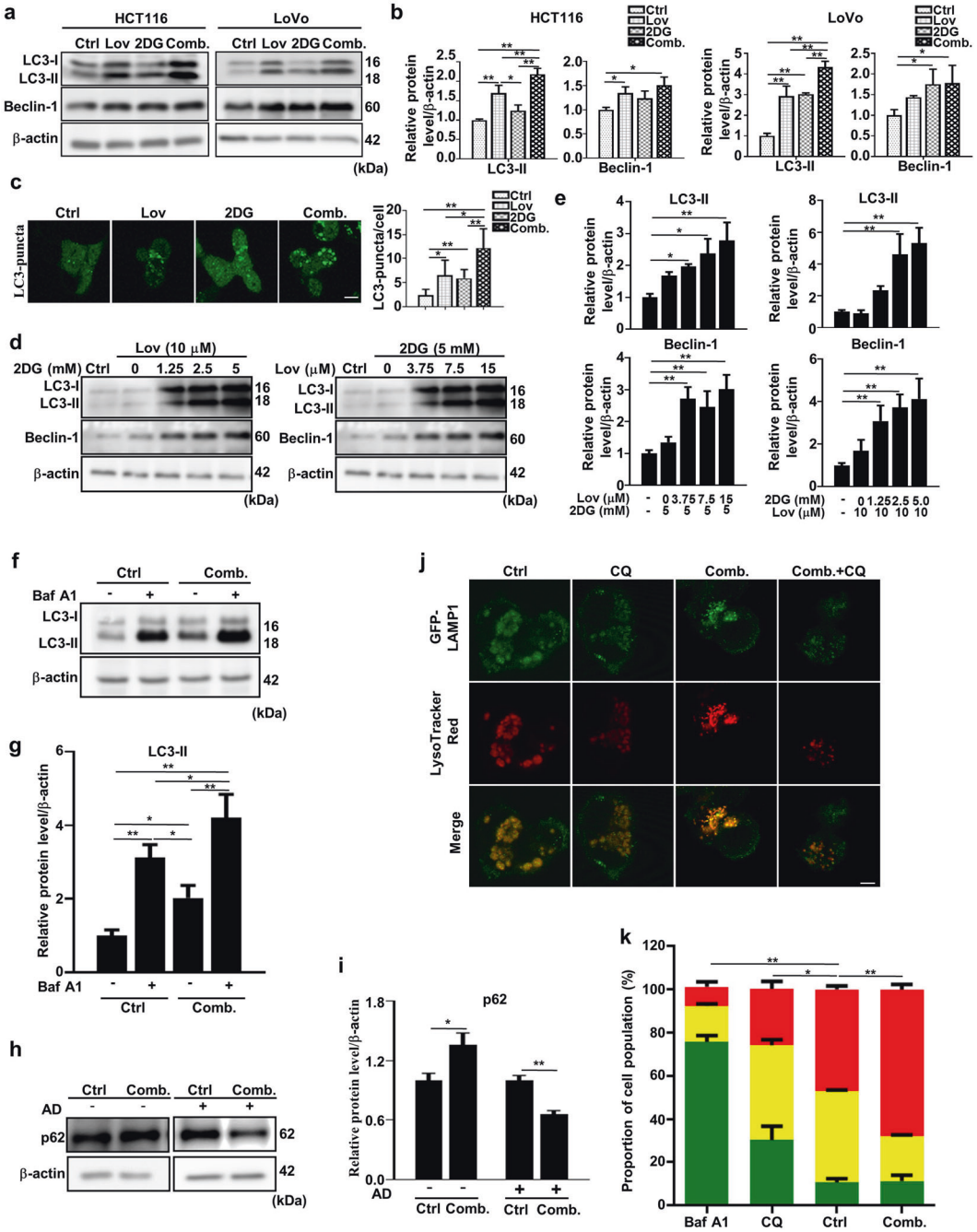

Fig. 5 The combination of lovastatin and 2DG enhances autophagic flux. The combination of lovastatin and 2DG increases autophagic flux. **a** Representative immunoblots of LC3 and Beclin-1 in HCT116 and LoVo cells after treatment with lovastatin (15 μM) and 2DG (5 mM) alone or in combination for 48 h. β-actin served as a loading control. **b** Quantified data of (**a**). **c** Cells transfected with the pEGFP-LC3 plasmid were analyzed for pEGFP-LC3 puncta formation in HCT116 cells after treatment with lovastatin (15 μM) and 2DG (5 mM) alone or in combination for 48 h. Bar, 20 μm. **d** Representative immunoblots showing LC3 and Beclin-1 from HCT116 cells treated with either 2DG (5 mM) and different concentrations of lovastatin or lovastatin (15 μM) and different concentrations of 2DG for 48 h. **e** Quantified data of (**d**). **f** Representative immunoblots showing LC3 from HCT116 cells treated with either vehicle or the combination of lovastatin (15 μM) and 2DG (5 mM) for 20 h, followed by treatment with or without bafilomycin A1 (100 nM) for 4 h. **g** Quantified data of (**f**). **h** HCT116 cells were treated with either vehicle or a combination of lovastatin (15 μM) and 2DG (5 mM) in the presence or absence of actinomycin D (8 μM) for 24 h. Representative immunoblots of p62 protein levels. β-actin served as a loading control. **i** Quantified data of (**h**). **j** HCT116 cells were transduced with LAMP1-GFP and cultured for 24 h. Then, the cells were treated with vehicle, CQ (20 μM), a combination of lovastatin (15 μM) and 2DG (5 mM) or lovastatin + 2DG + CQ for 48 h. The cells were stained with 75 nM LysoTracker Red and imaged. Bar, 10 μm. **k** HCT116 cells expressing an autophagic flux reporter (AFR) were generated by ectopic expression of a chimeric fusion protein composed of pHluorin-mKate2-hLC3. The increased ratio of red (mKate2):green (pHluorin) fluorescence measured by flow cytometry is an indication of increased autophagic flux. Autophagic flux in HCT116 cells was also measured by flow cytometry following 48 h of treatment with either vehicle or the combination of lovastatin (15 μM) and 2DG (5 mM) and bafilomycin A1 (100 nM) as a negative control for 4 h (*$P < 0.05$, **$P < 0.01$ versus high (red)). All data are from at least three independent experiments. *$P < 0.05$, **$P < 0.01$.

the combination of lovastatin and 2DG was found to increase p62 levels (Fig. 5h, i). Since degradation of p62 can be masked by the transcriptional upregulation of the protein even in the presence of activated autophagic flux in some circumstances [37], we measured p62 levels in the presence of AD, a potent transcription inhibitor. As shown in Fig. 5h and i, p62 was significantly degraded in the combination treatment group.

Furthermore, to determine whether lysosomal function was affected by the combination treatment, we used the acidotropic fluorescence dye LysoTracker Red to measure the lysosomal pH in HCT116 cells expressing the fusion protein of lysosomal-associated membrane protein 1 (LAMP-1) with GFP. CQ neutralized the lysosomal pH and thus reduced the fluorescence of LysoTracker Red. In contrast, the combination of lovastatin and 2DG slightly increased the fluorescence intensity, an effect that was almost entirely blocked by CQ (Fig. 5j). To confirm that the combination treatment promotes autophagy, HCT116 cells were engineered to express a chimeric AFR protein consisting of pHluorin, mKate2, and LC3. The increased ratio between the pH-insensitive red fluorescence emitted by mKate2 and the pH-sensitive green fluorescence emitted by pHluorin indicated that the autophagic flux was enhanced [38]. In contrast to Baf A1 and CQ, which dramatically suppressed the ratio of mKate2: pHluorin, the combination of lovastatin and 2DG significantly increased the ratio in HCT116 AFR cells (Fig. 5k).

The inhibition of autophagy increases the vulnerability of HCT116 and LoVo cells to combined treatment with lovastatin and 2DG

Autophagy is a survival mechanism mobilized by cells facing metabolic stress. Therefore, we postulated that the inhibition of autophagy would increase the susceptibility of KRAS-mutant cells to treatment with the combination of lovastatin and 2DG. Indeed, the lysosomal acidification inhibitor CQ significantly decreased cell viability in the combination group, as measured by SRB assay (Fig. 6a). A slight but not significant decrease in cells treated with the individual agents may have been caused by the relatively weak autophagic flux, as exemplified by the difference in LC3II levels compared to the level in the combination group (Figs. 5a and 6a). When tested by clonogenic assay, a more sensitive approach, supplementation of CQ was found to significantly inhibit colony numbers in all treatment groups, with the combination treatment exhibiting the most dramatic inhibition (Fig. 6b, c). In contrast, CQ did not potentiate the inhibition of cell proliferation by treatments with individual agents or the drug combination in KRAS wild-type HCT-8 cells (Supplementary Fig. S1b) and normal colonic epithelial CCD-841-CoN cells (Supplementary Fig. S1d).

Finally, we measured the anticancer activity of lovastatin, 2DG, and HCQ in different regimens using a HCT116 xenograft model. One of the major concerns is the safety of an increased number of drugs, which may induce side effects. Although the body weights of the mice treated with lovastatin alone, the combination of lovastatin and 2DG, HCQ alone, and HCQ in combination with lovastatin and 2DG were slightly (but not significantly) decreased at the end of the experiments, all the animals were in good health and exhibited normal physical activity levels (Fig. 6d). Single-agent treatments elicited no noticeable effect, except lovastatin, which modestly inhibited the growth of the xenografts (Fig. 6e, f). The lack of an in vivo effect of 2DG and HCQ mono in clinical studies was reported [5, 6, 39]. Notably, the combination of lovastatin and 2DG significantly reduced tumor volume ($P < 0.01$), which is consistent with the in vitro results. Surprisingly, when these two drugs were combined with HCQ, there was a dramatic regression in the growth of the xenografts ($P < 0.05$).

DISCUSSION

Glucose dependence is the foundation for a promising therapeutic regimen for RAS-mutant CRCs. However, monotherapy with the glycolysis inhibitor 2DG has shown limited clinical effectiveness, possibly due to the compensatory increase in OXPHOS metabolism [5, 6]. In this study, we measured the anticancer activity of the OXPHOS inhibitor lovastatin in combination with 2DG in HCT116 and LoVo cell lines with KRAS mutations. Compared to the treatments with single agents, the combination treatment elicited a more profound effect on cell proliferation (Fig. 1), the induction of apoptosis (Fig. 2), cell cycle arrest (Fig. 3), and autophagic flux (Fig. 5). Mechanistically, the combination treatment exhibited a synergistic effect on previously identified activities of the single agents, including the inhibitory effect of statins on OXPHOS (Fig. 4 a–d) [30], the inhibitory effect of 2DG on metabolism (Fig. 4 a–d) [31], and the inhibitory effect of statins/2DG on the RAS signaling pathway (Fig. 2 e, f) [40–42]. The synergistic effects on cell metabolism included depletion of ATP, activation of AMPK, and inhibition of mTOR, subsequently leading to the suppression of cell proliferation and the activation of autophagic flux. The synergistic effect on the RAS signaling pathway resulted in the induction of apoptosis and the activation of autophagy (Fig. 6g).

Autophagy, as a stress-responsive mechanism, provides substrates for glycolysis and OXPHOS to protect cells from death [43]. Recently, the inhibition of KRAS was reported to significantly attenuate both glycolytic flux and OXPHOS activity in KRAS-mutant cancer cells, leading to enhanced sensitivity to autophagy inhibition induced with CQ/HCQ [44, 45]. Our results further emphasized this point (Fig. 6g). Targeting these metabolic pathways with one or two agents (but not three) has been extensively investigated for RAS-driven tumors [46]. The mutual interplay between these metabolic pathways provides the rationale for the use of combinations of 2DG, statins, and HCQ in KRAS-mutant colon cancers, which has not been evaluated to date.

Treatment with lovastatin or 2DG alone inhibited cell proliferation to a similar degree in the KRAS wild-type HCT-8 cells and KRAS-mutant CRC cell lines. However, no synergistic effect was observed when the two drugs were used in combination (Supplementary Fig. S1a). In CCD-841-CoN normal human colonic epithelial cells, neither the single-agent nor combination treatments significantly affected cell growth (Supplementary Fig. S1c). More importantly, when autophagy was inhibited by CQ, cell growth was no longer affected (Supplementary Fig. S1b, d). These data indicate that treatment with a combination of a statin and 2DG selectively affects KRAS-mutant CRC cells. Additionally, increased cell susceptibility was induced by the inhibition of autophagy following treatment with the combination of drugs only in the KRAS-mutant CRC cells. However, to make a more robust conclusion, the effects of these treatments should be tested in additional CRC cell lines with different KRAS backgrounds, as well as in paired cell lines with genetically modified KRAS genes.

The results of this study should be interpreted by considering the doses of lovastatin and 2DG used in the experiments. While the concentration of statins in human serum is in the nM range, the concentrations used in cancer research in vitro range from 1 to 200 μM, as reviewed by Stamm et al. [47]. The clinically achievable concentration of 2DG is 3–4 mM [48], and 5 mM is relatively high but is not uncommon for use in vitro studies [31, 49]. For cell experiments, we chose the concentrations of lovastatin (15 μM) and 2DG (5 mM) close to the IC_{50} values obtained with the cell proliferation assay (Fig. 1a), which may vary between cell lines. For animal studies, the dose of 25 mg/kg every 2 d was based on previous studies [50, 51]. As summarized by Pecoraro et al., statin doses used in most rodent studies range between 1 and 100 mg/kg [52], which is much higher than the doses administered to patients. However, the higher doses used in rodents likely reflect the pharmacodynamic resistance to the pharmacological effect of statins in rodents [53].

The autophagy assays should be interpreted with caution since these measures can be context-dependent, and multiple assays

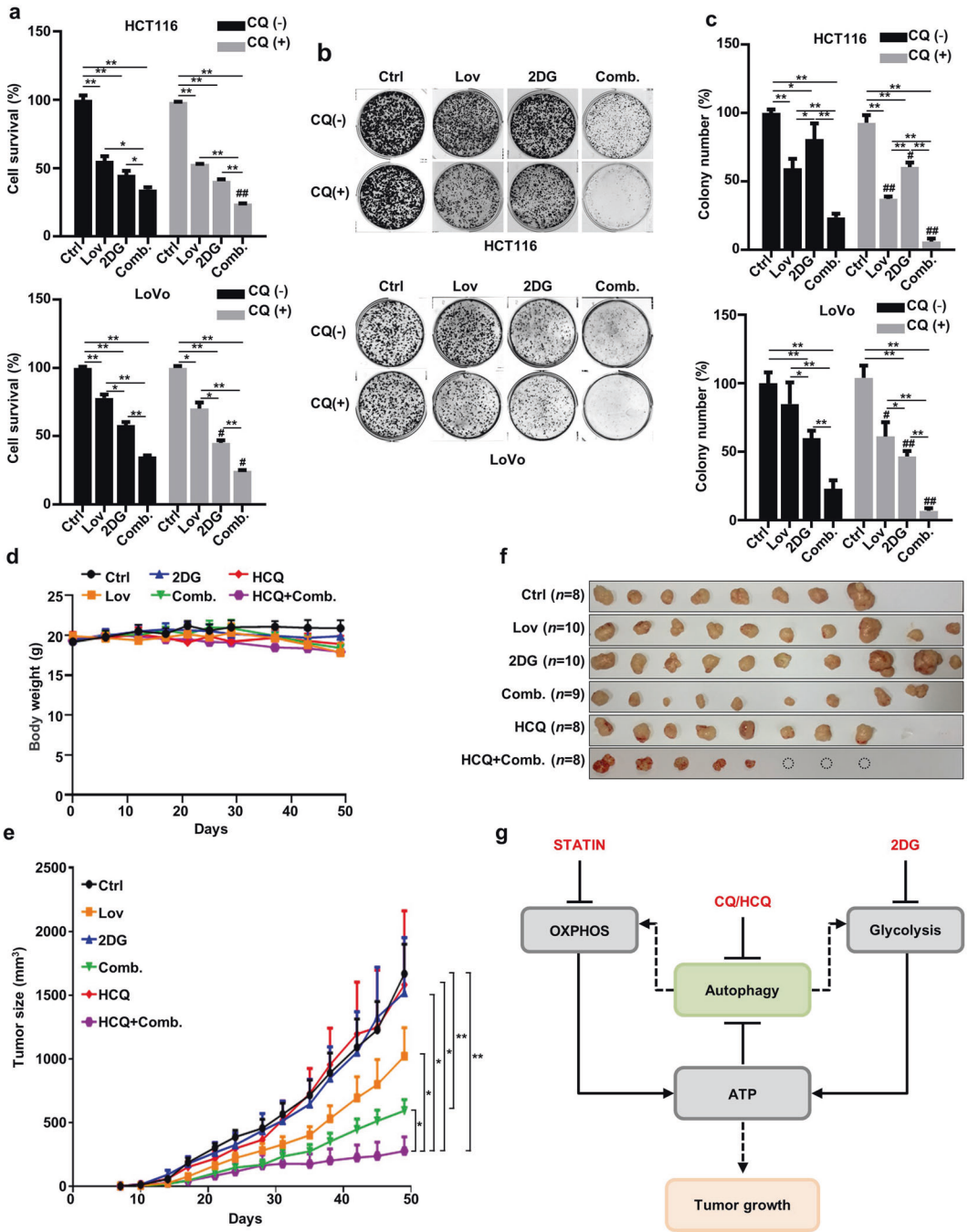

Fig. 6 The inhibition of autophagy increases the vulnerability of HCT116 cells and LoVo cells to combined treatment with lovastatin and 2DG. a HCT116 and LoVo cells were treated with lovastatin (15 μM) and 2DG (5 mM) alone or in combination for 72 h in the presence or absence of chloroquine (CQ) (6.25 μM), and cell proliferation was determined ($n = 3$) ($^{*}P < 0.05$, $^{**}P < 0.01$. $^{\#}P < 0.05$, $^{\#\#}P < 0.01$ versus indicated treatment group in the absence of CQ). **b** Colony formation of HCT116 and LoVo cells treated with lovastatin (5 μM) and 2DG (2 mM) alone or in combination in the presence or absence of CQ (400 nM) for 10 d. **c** Quantified data of (**b**) ($n = 4$). ($^{*}P < 0.05$, $^{**}P < 0.01$. $^{\#}P < 0.05$, $^{\#\#}P < 0.01$ versus indicated treatment group in the absence of CQ). **d** HCT116 cells were injected subcutaneously into each hind limb of nude mice, and hydroxychloroquine (HCQ) (80 mg/kg every 2 d), lovastatin (25 mg/kg every 2 d), 2DG (5 mg/kg every 2 d), Comb. (lovastatin + 2DG) and HCQ + Comb. were administered orally. Ctrl $n = 8$, lovastatin $n = 10$, 2DG $n = 10$, HCQ $n = 8$, Comb. $n = 9$, HCQ + Comb. $n = 8$. Data were shown as the means ± SEM. **e** Tumor size in the mice shown in (**d**). $^{*}P < 0.05$, $^{**}P < 0.01$. Data are shown as the means ± SEM. **f** Tumors excised from mice in (**d**), and the dotted circle represents the tumor that completely disappeared after treatment. **g** Schematic representation of the combined effect of lovastatin and 2DG showing increased susceptibility of HCT116 cells to autophagy inhibition.

(instead of a single method) should be used to evaluate autophagy [36]. Therefore, we measured the protein level of LC3II, as well as the protein levels of Beclin-1 and p62, well-known markers of autophagy. However, the p62 levels were unexpectedly increased following treatment with the combination of lovastatin and 2DG, likely as a result of enhanced protein transcription (Fig. 5h). p62 has been shown to regulate energy metabolism [54, 55]. However, how energy depletion by the simultaneous inhibition of glycolysis and OXPHOS affects p62 transcription remains to be elucidated. We also detected autophagosome

formation, as indicated by LC3 puncta (Fig. 5c), identified functional lysosomes using the acidotropic fluorescence dye LysoTracker Red (Fig. 5j), and measured autophagic flux using a chimeric AFR system (Fig. 5k). The set of results firmly proved the induction of autophagic flux by treatment with a combination of lovastatin and 2DG in RAS-mutant CRC cells.

Statins have been shown to suppress glycolysis by inhibiting glucose transporter 1 (GLUT1)-mediated glucose uptake [56]. However, the findings are complicated and controversial. While a number of studies have demonstrated no effect of statins on glycolysis [57, 58], our group has recently shown that statins stimulate glycolysis through the regulation of the p53/β-enolase axis [30]. This discrepancy may be the result of differences in the cell lines, methods, and experimental designs used in various studies.

In contrast to glycolysis, OXPHOS is a relatively new target for cancer treatments [59]. The antidiabetic drug metformin is the most widely recognized OXPHOS inhibitor, with antitumor effects demonstrated in clinical studies [60]. Statins affect mitochondrial function through multiple mechanisms but have attracted far less attention to date. Even though metformin is able to activate AMPK, it inhibits 2DG-induced autophagy [61]. In contrast, lovastatin was found to induce autophagy synergistically when used in combination with 2DG (Fig. 5). We therefore expect that the combination of 2DG with statins may increase the susceptibility of cancer cells to autophagy inhibition compared to the combination of 2DG with metformin.

In summary, our study highlights a promising regimen composed of the glycolysis inhibitor 2DG, OXPHOS inhibitor lovastatin, and autophagy inhibitor CQ/HCQ for the treatment of RAS-mutant CRCs. Further evaluation of the effectiveness of the combination treatment through clinical studies is warranted.

ACKNOWLEDGEMENTS

This work was funded by the Science and Technology Development Fund, Macau SAR, China (File no. 0036/2020/A1, 0013/2019/A1 and 0039/2020/A).

AUTHOR CONTRIBUTIONS

XMH and WZM conceived and planned the experiments; XMH, JJH, JJD, NZ, ZL, and YY performed the experiments; XMH, FFZ, BWZ, YFS, ZH, XQ, JHC, QYL and WJL analyzed the data; XMH and WZM wrote the manuscript.

ADDITIONAL INFORMATION

Supplementary information The online version contains supplementary material available at https://doi.org/10.1038/s41401-021-00612-9.

Competing interests: The authors declare no competing interests.

REFERENCES

1. Bray F, Ferlay J, Soerjomataram I, Siegel RL, Torre LA, Jemal A. Global cancer statistics 2018: GLOBOCAN estimates of incidence and mortality worldwide for 36 cancers in 185 countries. CA Cancer J Clin. 2018;68:394–424.
2. Serebriiskii IG, Connelly C, Frampton G, Newberg J, Cooke M, Miller V, et al. Comprehensive characterization of RAS mutations in colon and rectal cancers in old and young patients. Nat Commun. 2019;10:1–12.
3. Mármol I, Sánchez-de-Diego C, Pradilla Dieste A, Cerrada E, Rodriguez Yoldi MJ. Colorectal carcinoma: a general overview and future perspectives in colorectal cancer. Int J Mol Sci. 2017;18:197.
4. Kimmelman AC. Metabolic dependencies in RAS-driven cancers. Clin Cancer Res. 2015;2:1828–34.
5. Stein M, Lin H, Jeyamohan C, Dvorzhinski D, Gounder M, Bray K, et al. Targeting tumor metabolism with 2-deoxyglucose in patients with castrate-resistant prostate cancer and advanced malignancies. Prostate. 2010;70:1388–94.
6. Raez LE, Papadopoulos K, Ricart AD, Chiorean EG, DiPaola RS, Stein MN, et al. A phase I dose-escalation trial of 2-deoxy-D-glucose alone or combined with docetaxel in patients with advanced solid tumors. Cancer Chemother Pharmacol. 2013;71:523–30.
7. Sanderson SM, Locasale JW. Revisiting the Warburg effect: some tumors hold their breath. Cell Metab. 2018;28:669–70.
8. Villanueva MT. Metabolic synthetic lethality. Nat Rev Drug Discov. 2018;17:543.
9. Jia D, Lu M, Jung KH, Park JH, Yu L, Onuchic JN, et al. Elucidating cancer metabolic plasticity by coupling gene regulation with metabolic pathways. Proc Natl Acad Sci USA. 2019;116:3909–18.
10. Cheong JH, Park ES, Liang J, Dennison JB, Tsavachidou D, Nguyen-Charles C, et al. Dual inhibition of tumor energy pathway by 2-deoxyglucose and metformin is effective against a broad spectrum of preclinical cancer models. Mol Cancer Ther. 2011;10:2350–62.
11. Bizjak M, Malavašič P, Dolinar K, Pohar J, Pirkmajer S, Pavlin M. Combined treatment with Metformin and 2-deoxy glucose induces detachment of viable MDA-MB-231 breast cancer cells in vitro. Sci Rep. 2017;7:1–14.
12. Mert I, Chhina J, Allo G, Dai J, Seward S, Carey MS, et al. Synergistic effect of MEK inhibitor and metformin combination in low grade serous ovarian cancer. Gynecol Oncol. 2017;146:319–26.
13. Mamtani R, Lewis JD, Scott FI, Ahmad T, Goldberg DS, Datta J, et al. Disentangling the association between statins, cholesterol, and colorectal cancer: a nested case-control study. PLoS Med. 2016;13:e1002007.
14. Ungefroren H, Witte D, Lehnert H. The role of small GTPases of the Rho/Rac family in TGF-β-induced EMT and cell motility in cancer. Dev Dyn. 2018;247:451–61.
15. Kuzu OF, Noory MA, Robertson GP. The role of cholesterol in cancer. Cancer Res. 2016;76:2063–70.
16. Urbano F, Bugliani M, Filippello A, Scamporrino A, Di Mauro S, Di, et al. Atorvastatin but not pravastatin impairs mitochondrial function in human pancreatic islets and rat β-cells. Direct effect of oxidative stress. Sci Rep. 2017;7:11863.
17. Singh F, Zoll J, Duthaler U, Charles AL, Panajatovic MV, Laverny G, et al. PGC-1β modulates statin-associated myotoxicity in mice. Arch Toxicol. 2019;93:487–504.
18. Levy JMM, Towers CG, Thorburn A. Targeting autophagy in cancer. Nat Rev Cancer. 2017;17:528–42.
19. Levy JMM, Thorburn A. Autophagy in cancer: moving from understanding mechanism to improving therapy responses in patients. Cell Death Differ. 2020;27:843–57.
20. Xu R, Ji Z, Xu C, Zhu J. The clinical value of using chloroquine or hydroxychloroquine as autophagy inhibitors in the treatment of cancers: a systematic review and meta-analysis. Medicine (Baltimore). 2018;97:e12912.
21. Shen Y, Wang C, Ren Y, Ye J. A comprehensive look at the role of hyperlipidemia in promoting colorectal cancer liver metastasis. J Cancer. 2018;9:2981–6.
22. Lin W, Huang J, Yuan Z, Feng S, Xie Y, Ma W. Protein kinase C inhibitor chelerythrine selectively inhibits proliferation of triple-negative breast cancer cells. Sci Rep. 2017;7:2022.
23. Lin W, Huang J, Liao X, Yuan Z, Feng S, Xie Y, et al. Neo-tanshinlactone selectively inhibits the proliferation of estrogen receptor positive breast cancer cells through transcriptional down-regulation of estrogen receptor alpha. Pharmacol Res. 2016;111:849–58.
24. Chou TC. Theoretical basis, experimental design, and computerized simulation of synergism and antagonism in drug combination studies. Pharmacol Rev. 2006;58:621–81.
25. Motawe ZY, Farsaei F, Abdelmaboud SS, Cuevas J, Breslin JW. Sigma-1 receptor activation-induced glycolytic ATP production and endothelial barrier enhancement. Microcirculation. 2020;27:e12620.
26. Spiegel J, Cromm PM, Zimmermann G, Grossmann TN, Waldmann H. Small-molecule modulation of Ras signaling. Nat Chem Biol. 2014;10:613–22.
27. Evan GI, Vousden KH. Proliferation, cell cycle and apoptosis in cancer. Nature. 2001;411:342–8.
28. Lew DJ, Kornbluth S. Regulatory roles of cyclin dependent kinase phosphorylation in cell cycle control. Curr Opin Cell Biol. 1996;8:795–804.
29. Icard P, Fournel L, Wu Z, Alifano M, Lincet H. Interconnection between metabolism and cell cycle in cancer. Trends Biochem Sci. 2019;44:490–501.
30. Huang J, Du J, Lin W, Long Z, Zhang N, Huang X, et al. Regulation of lactate production through p53/β-enolase axis contributes to statin-associated muscle symptoms. EBioMed. 2019;45:251–60.
31. Robinson G, Dinsdale D, Macfarlane M, Cain K. Switching from aerobic glycolysis to oxidative phosphorylation modulates the sensitivity of mantle cell lymphoma cells to TRAIL. Oncogene. 2012;31:4996–5006.
32. Hardie DG, Ross FA, Hawley SA. AMPK: a nutrient and energy sensor that maintains energy homeostasis. Nat Rev Mol Cell Biol. 2012;13:251–62.
33. Lin SC, Hardie DG. AMPK: sensing glucose as well as cellular energy status. Cell Metab. 2018;27:299–313.
34. Saxton RA, Sabatini DM. mTOR signaling in growth, metabolism, and disease. Cell. 2017;168:960–76.
35. Giammarioli AM, Gambardella L, Barbati C, Pietraforte D, Tinari A, Alberton M, et al. Differential effects of the glycolysis inhibitor 2-deoxy-D-glucose on the activity of pro-apoptotic agents in metastatic melanoma cells, and induction of a cytoprotective autophagic response. Int J Cancer. 2012;131:E337–47.

36. Klionsky DJ, Abdelmohsen K, Abe A, Abedin MJ, Abeliovich H, Acevedo Arozena A, et al. Guidelines for the use and interpretation of assays for monitoring autophagy. Autophagy. 2016;12:1–222.
37. Zheng Q, Su H, Ranek MJ, Wang X. Autophagy and p62 in cardiac proteinopathy. Circ Res. 2011;109:296–308.
38. Tanida I, Ueno T, Uchiyama Y. A super-ecliptic, pHluorin-mKate2, tandem fluorescent protein-tagged human LC3 for the monitoring of mammalian autophagy. PLoS One. 2014;9:e110600.
39. Wolpin BM, Rubinson DA, Wang X, Chan JA, Cleary JM, Enzinger PC, et al. Phase II and pharmacodynamic study of autophagy inhibition using hydroxychloroquine in patients with metastatic pancreatic adenocarcinoma. Oncologist. 2014;19:637–8.
40. Chen J, Bi H, Hou J, Zhang X, Zhang C, Yue L, et al. Atorvastatin overcomes gefitinib resistance in KRAS mutant human non-small cell lung carcinoma cells. Cell Death Dis. 2013;4:e814.
41. Park IH, Kim JY, Jung JI, Han JY. Lovastatin overcomes gefitinib resistance in human non-small cell lung cancer cells with K-Ras mutations. Invest N Drugs. 2010;28:791–9.
42. Kovács K, Decatur C, Toro M, Pham DG, Liu H, Jing Y, et al. 2-deoxy-glucose downregulates endothelial AKT and ERK via interference with N-Linked glycosylation, induction of endoplasmic reticulum stress, and GSK3β activation. Mol Cancer Ther. 2016;15:264–75.
43. Shen S, Codogno P. The role of autophagy in cell death. In: Hayat MA, editor. Autophagy: cancer, other pathologies, inflammation, immunity, infection, and aging. San Diego: Academic Press; 2016. p139–54.
44. Bryant KL, Stalnecker CA, Zeitouni D, Klomp JE, Peng S, Tikunov AP, et al. Combination of ERK and autophagy inhibition as a treatment approach for pancreatic cancer. Nat Med. 2019;25:628–40.
45. Kinsey CG, Camolotto SA, Boespflug AM, Guillen KP, Foth M, Truong A, et al. Protective autophagy elicited by RAF→ MEK→ ERK inhibition suggests a treatment strategy for RAS-driven cancers. Nat Med. 2019;25:620–7.
46. Ryan MB, Corcoran RB. Therapeutic strategies to target RAS-mutant cancers. Nat Rev Clin Oncol. 2018;15:709–20.
47. Stamm JA, Ornstein DL. The role of statins in cancer prevention and treatment. Oncology (Williston Park). 2005;19:739–50.
48. Mohanti BK, Rath GK, Anantha N, Kannan V, Das BS, Chandramouli BA, et al. Improving cancer radiotherapy with 2-deoxy-D-glucose: phase I/II clinical trials on human cerebral gliomas. Int J Radiat Oncol Biol Phys. 1996;35:103–11.
49. Goldberg L, Israeli R, Kloog Y. FTS and 2-DG induce pancreatic cancer cell death and tumor shrinkage in mice. Cell Death Dis. 2012;3:e284.
50. Ni T, He Z, Dai Y, Yao J, Guo Q, Wei L. Oroxylin A suppresses the development and growth of colorectal cancer through reprogram of HIF1α-modulated fatty acid metabolism. Cell Death Dis. 2017;8:e2865.
51. Shibata MA, Ito Y, Morimoto J, Otsuki Y. Lovastatin inhibits tumor growth and lung metastasis in mouse mammary carcinoma model: a p53-independent mitochondrial-mediated apoptotic mechanism. Carcinogenesis. 2004;25:1887–98.
52. Pecoraro V, Moja L, Dall'Olmo L, Cappellini G, Garattini S. Most appropriate animal models to study the efficacy of statins: a systematic review. Eur J Clin Invest. 2014;44:848–71.
53. Björkhem-Bergman L, Lindh JD, Bergman P. What is a relevant statin concentration in cell experiments claiming pleiotropic effects? Br J Clin Pharmcol. 2011;72:164–5.
54. Chen K, Zeng J, Xiao H, Huang C, Hu J, Yao W, et al. Regulation of glucose metabolism by p62/SQSTM1 through HIF1α. J Cell Sci. 2016;129:817–30.
55. Müller TD, Lee SJ, Jastroch M, Kabra D, Stemmer K, Aichler M, et al. p62 Links β-adrenergic input to mitochondrial function and thermogenesis. J Clin Invest. 2013;123:469–78.
56. Malenda A, Skrobanska A, Issat T, Winiarska M, Bil J, Oleszczak B, et al. Statins impair glucose uptake in tumor cells. Neoplasia. 2012;14:311–23.
57. Christie CF, Fang D, Hunt EG, Morris ME, Rovini A, Heslop KA, et al. Statin-dependent modulation of mitochondrial metabolism in cancer cells is independent of cholesterol content. FASEB J. 2019;33:8186–201.
58. Kuzyk CL, Anderson CC, Roede JR. Simvastatin induces delayed apoptosis through disruption of glycolysis and mitochondrial impairment in neuroblastoma cells. Clin Trans Sci. 2020;13:563–72.
59. Ashton TM, McKenna WG, Kunz-Schughart LA, Higgins GS. Oxidative phosphorylation as an emerging target in cancer therapy. Clin Cancer Res. 2018;24:2482–90.
60. Bridges HR, Jones AJ, Pollak MN, Hirst J. Effects of metformin and other biguanides on oxidative phosphorylation in mitochondria. Biochem J. 2014;462:475–87.
61. Ben Sahra I, Tanti JF, Bost F. The combination of metformin and 2 deoxyglucose inhibits autophagy and induces AMPK-dependent apoptosis in prostate cancer cells. Autophagy. 2010;6:670–1.